Study on the Al₂O₃/Fe-Al intermetallic duplex coating prepared with a combined technique of electro-spark deposition and micro-arc oxidation on steel

A. Çakir[1]*, K. Korkmaz[1], E. S. Kayali[2]

[1] *Gebze Technical University, Department of Materials Science and Engineering, TR-41400 Gebze, Kocaeli, Turkey*
[2] *Haliç University, Department of Industrial Engineering, Kağıthane, TR-34083 Istanbul, Turkey*

Abstract

In the present study, an electro-spark deposition method was applied to obtain a corrosion resistant FeAl-based layer onto the steel surface. In this context, firstly the pulse parameters of deposition process were optimized and among all the parameters, 200 A and 50 µs were determined as the best ones. Then, micro-arc oxidation technique was performed to enhance tribological properties of the FeAl-coated steel samples in the electrolyte solution which consisted of Na_3PO_4 and $NaAlO_2$. The coated samples were characterized by SEM/EDX and XRD examinations. The results showed that the duplex coating was composed of Al_2O_3 and $FeAl_2$ phases while FeAl, Fe_2Al_5, and Fe_3Al phases were present in the ESD coating. Mechanical properties of duplex coatings on the steel substrate were significantly improved, and so the microhardness of micro-arc oxidation and electro-spark deposition coatings was about 4 and 5 times of the steel substrate microhardness, respectively. Moreover, the corrosion resistance of the coatings was determined as well. Its value for the micro-arc oxidation and electro-spark deposition coating was about 40 and 20 % better than that for the substrate steel, respectively.

K e y w o r d s: electro-spark deposition, micro-arc oxidation, duplex coating, Fe-Al intermetallic

1. Introduction

Today, the steel is still used in a wide range of the industrial applications due to its outstanding properties such as a high strength and excellent mechanical characteristics. In particular, low carbon steels have an important position in structural applications since their production and manufacturing cost is lower than that for high carbon steels or non-ferrous alloys [1]. However, the poor oxidation and corrosion resistance in high-temperature environments and aggressive corrosive media, respectively, could limit their access to possible broader applications. Moreover, the scaling always takes place on their surface after and/or during manufacturing process [2–5].

Therefore, many researchers have investigated ways to improve their properties and thus, most of them have applied the addition of alloying elements or surface treatments onto the steel surfaces. Especially, the formation of FeAl-intermetallics such as FeAl, Fe_3Al, and Fe_2Al_5 on the steel surfaces could be a promising method to solve the present problems, because Al and its alloys have excellent corrosion resistance and also they could present a possibility to form a protective coating such as alumina for applications at high temperature. In previous studies, some methods have been applied to form Al-based coating on the steel surface such as weld-overlay [6, 7], pack cementation [8], thermal spray technique [9–11], high-velocity oxyfuel (HVOF) [12], hot dipping [13], chemical vapor deposition [14], ion vapor deposition and slurry [15, 16].

However, in most of these methods, it has not been easy to develop a coating, and they have been high-cost coating processes. On the other hand, the electro-spark deposition (ESD) technique offers some unique advantages relative to these methods [17–20]. In a previous study [21], Frangini et al. have reported that the

Table 1. Chemical composition of St37 steel substrate (wt.%)

Alloy elements	C	Mn	P	S	Cr	Al	Fe
Chemical composition	0.217	0.426	0.026	0.022	0.064	0.017	Bal.

Table 2. Chemical composition of aluminum treating electrode (wt.%)

Alloy elements	Si	Fe	Mg	Zn	Ti	B	Ca	Na	Al
Chemical composition	0.085	0.228	0.0039	0.0010	0.0020	0.0021	0.0054	0.0012	Bal.

FeAl coating which was coated on 316L stainless steel surface had a higher hardness and corrosion resistance than the substrate. Johnson stated that Fe_3Al alloys indicated better mechanical properties than FeAl in structure applications. On the other hand, FeAl could be chosen in the applications that required high aluminum content for corrosion resistance [22].

Furthermore, alumina coating is a very effective technique for the enhancement of tribological properties and corrosion behavior of metallic surfaces. Micro-arc oxidation (MAO), also known as plasma electrolytic oxidation (PEO), is novel technique to produce hard ceramic coatings on valve metals such as Al, Ti, Mg, Zr, etc. and their alloys [23, 24]. In addition to that, this technique may offer the opportunity to form an oxide layer that strongly adheres to substrate materials with open cell structure or to achieve duplex coatings [25, 26].

In this study, ESD method was performed to achieve iron-aluminides coating on the steel surface which is suitable for the next MAO process. Furthermore, ESD technique enables us to create a strong metallurgical bonding between the coating and substrate. Then, to develop tribological and corrosion properties of the present iron-aluminides coating on the steel surface, an alumina layer with high hardness and enhanced corrosion resistance was obtained by using MAO process. The properties of this duplex coating are investigated and characterized in detail.

2. Experimental procedure

2.1. ESD and MAO process devices

In the ESD coating experiments, a special unit was employed. Its power consumption was 1.25 kW, and the output of stabilized voltage was constant at 45 V. It has the capability to generate pulses with a given energy and shape form. The installation is run with a special computer program [20]. The MAO process equipment consisted of bipolar pulsed AC power (100 kW) source, a stainless steel container as the electrolyte cell, and a stirring and cooling system [25].

2.2. Materials and methods

The aluminum rod with a radius of 4 mm and St37 substrates were used in the ESD coating process as a treating electrode and workpiece, respectively. Tables 1 and 2 present the chemical composition of St37 steel and Al rod. St37 steel workpiece analysis was obtained from the literature and the spectral analysis of the aluminum electrode was carried out by Ametek Spectro MAXx LMF14 device.

In the present study, the ESD process was conducted in the air with a series of rectangular pulses of a certain duration of 50 µs and with amplitudes of current 100–400 A. The pulse energies that correspond to these pulse parameters (amplitudes-duration) are presented in Table 3. To compare the results with each other in the experiments, the amount of electricity is kept constant as 1000 mC. Only five surfaces of the cubic samples ($1 cm^3$) to each processing condition were coated, and one surface was marked with numbers. One pass over the scanned (coated) area of $1 cm^2$ required approximately 1 min.

To achieve the duplex coatings and to form an oxide layer consisting of alumina (Al_2O_3) on iron aluminides (FeAl, Fe_3Al or Fe_2Al_5) ESD coated steel samples, the MAO process with bipolar impulses was applied at the second step. In the MAO process, cathodic and anodic voltages were performed while the ESD coated samples and the stainless steel container were used as the anode and cathode, respectively. The electrolyte solutions were prepared for MAO experiments. The electrolyte was composed of an aqueous solution of Na_3PO_4 and $NaAlO_2$ with concentrations of 4 and $8 g L^{-1}$, respectively. The treatment times and relevant voltages, which were used in the MAO experiments, are presented in Table 4.

2.3. Characterization of the coatings

The thickness of the ESD and duplex (ESD + MAO) coatings was measured on a Fischer Dualscope

Table 3. The parameters of rectangular pulse forms used in the ESD coating experiments

Parameter code	Coating pass number	Amplitude of current (A)	Duration time (µs)	Frequency (Hz)
R₁	4	100	50	242.4
R₂	4	200	50	116.3
R₃	4	300	50	75.8
R₄	4	400	50	54.7

Table 4. Process parameters of MAO coatings

	Voltage (V)	Current (A)	Duration time (µs)	Pause time (µs)	Duty ratio (%)
Anodic pulse	500	45	400	500	44.45
Cathodic pulse	200	75	700	500	58.33
Frequency (Hz)	50		Treatment time (min)		20

MP40 coating thickness gauge based on Eddy-Current method at five randomly selected locations. Scanning electron microscopy (SEM, Philips XL 30 SFEG) with energy dispersive X-ray microanalysis (EDX, EDAX Digital Control Software) and X-Ray Diffraction (XRD, Rigaku Dmax 2200) were performed to characterize and investigate the ESD and duplex coatings. X-ray diffraction pattern measurements were conducted in the range of 20° to 90°, at a scanning speed of 2° min⁻¹.

The Vickers microhardness was taken on the polished cross-section of the coatings. These measurements were made with a microhardness tester (Anton Paar MHT-10) at a load of 10 g and a loading time of 5 s. The metallographic analysis was carried out using an optical microscope (Zeiss Avio Imager M1m) equipped with Video Test Structure Software. Also, the adhesion strength of the coatings (ESD and duplex) to the substrate was determined by a Rockwell C test device (Zwick/Roell ZHR). The Rockwell C test was carried out by applying 150 kg load, and a diamond indenter with a radius of 500 µm was used at the tests.

The corrosion behavior of uncoated, ESD coated and duplex (ESD+MAO) coated steel samples was tested on a potentiometer device (Volta Lab PGZ 402 Potentiostat). The experiments were conducted in an aqueous electrolyte with distilled water and 3.5 % NaCl solution as corrosive media and a three-electrode corrosion cell as the test chamber. The potentiodynamic tests were performed in a polarization corrosion voltage from –500 to +500 mV at a sweeping rate of 1 mV s⁻¹ and at 25 ± 1 ℃.

3. Results and discussion
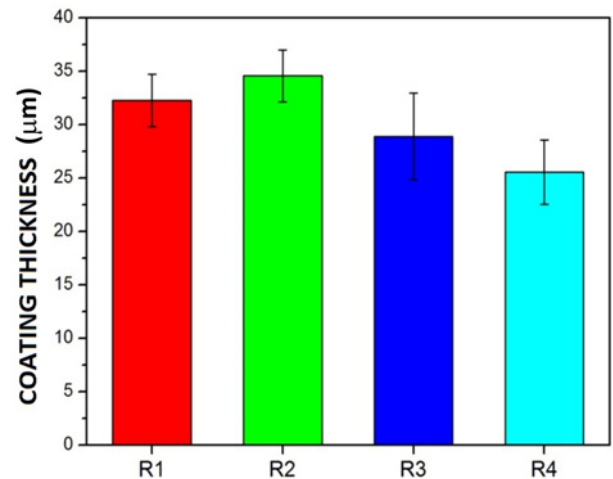
Plots of the change in the ESD coating thickness

Fig. 1. The thicknesses of the coatings for different pulse current amplitudes.

as a function of the different pulse sets are shown in Fig. 1. The pulse duration was fixed as 50 µs because the increase of coating thickness did not take place as expected by using longer pulse duration times. It was concluded that when ESD process was applied by pulses with longer duration times, it caused the aluminum electrode material to evaporate instead of its transfer to the substrate. The thickness of the coating which is produced by using rectangular pulses with the duration time of 50 µs increases as the amplitude of pulse current increases up to 200 A. A maximum value in the coating thickness could be achieved by using a pulse with the current amplitude of 200 A, and the duration time of 50 µs. In the ESD process, it is expected that if the amplitude of pulse current (or pulse energy) rises, the mass transfer to the substrate and the thickness of the coating increase. However, in the present study where pulses with high energy
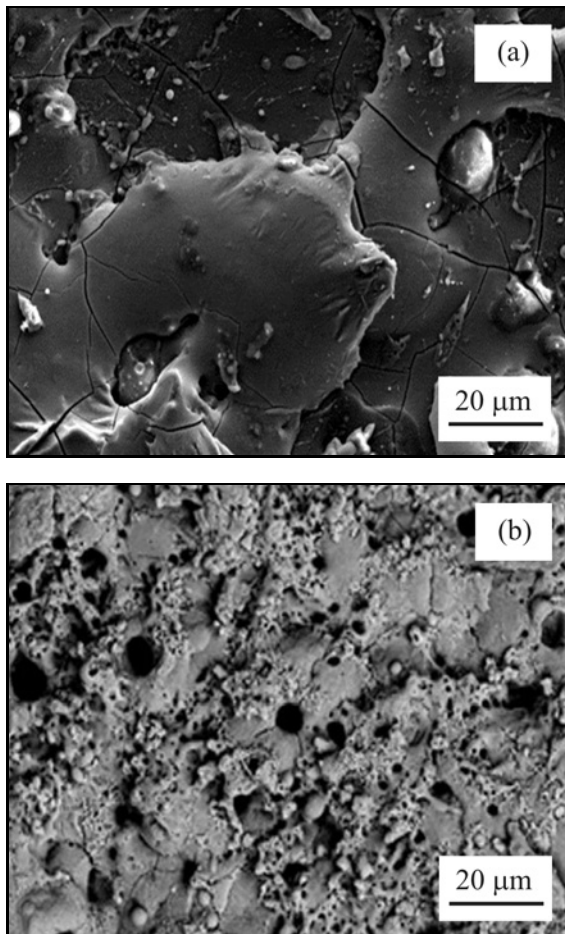
Fig. 2. Surface morphologies of a) ESD coating and b) duplex, ESD + MAO coatings.

Fig. 3. The cross-sectional image and line-scan EDX analysis of the duplex coating.

(or the current amplitude) are used, the erosive mass of aluminum electrode mostly vaporizes rather than transfers to the steel substrate due to the fact that the melting point of aluminum element is less than that of steel (or iron), approximately 2.5 times.

The surface morphology of the coating produced in the ESD technique by using the optimum pulse parameters is presented in Fig. 2a. It is known that the mechanism of material transfer from the electrode to the substrate is mostly globular mass transfer and this mechanism leads to a splash appearance on the coating surface when the ESD technique is performed in the air [17, 18]. As it can be seen, the coating surface is characterized as an irregular and rough view, due to this mass transfer mechanism. It is known that some failures (or defects) could form due to the over thermal energy which is caused by accumulating in the overheated mass transfer from treating electrode in the ESD coating with high energy pulses [27, 28]. In the present study, some microcracks are also visible on the coating surface in Fig. 2a. It can be concluded that the thermal expansion mismatch stress created
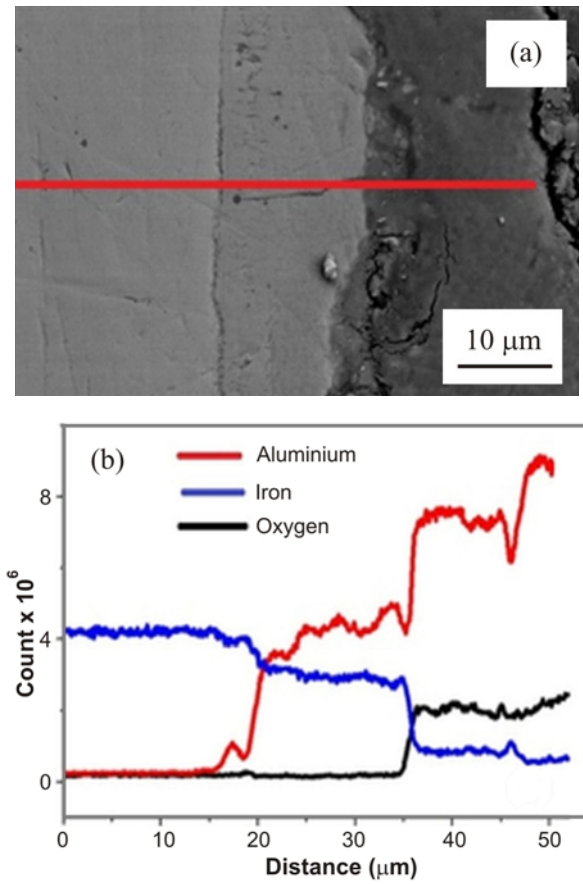
between the Al-Fe base alloyed coating and the steel substrate leads to the formation of these stress microcracks. Moreover, it can be deduced that a brittleness of the Fe-Al intermetallic compounds obtained on the surface could bring about the cracks. Figure 2b illustrates the surface morphology of the duplex coating. A lot of volcanic craters (or pores) which have been formed by micro arc discharge channels during the MAO process with different size and shape are randomly distributed all over the duplex coating surface.

A typical SEM micrograph for a cross-section of the duplex coating and also the distribution of elements in the coatings on the steel substrate are presented in Fig. 3. As expected, Fe and Al elements are present in the first layer which is an intermetallic alloy layer produced by ESD process. On the other hand, Fe, Al and also O elements are found in the second layer which is a ceramic layer produced by MAO process. As it is seen in Fig. 3, the thickness values of the ESD coating and duplex coating are approximately 15 and 20 μm, respectively. It was concluded that the thickness of the ESD coating layer decreased in the duplex coating after the MAO process due to the MAO layer development on the ESD coating layer.
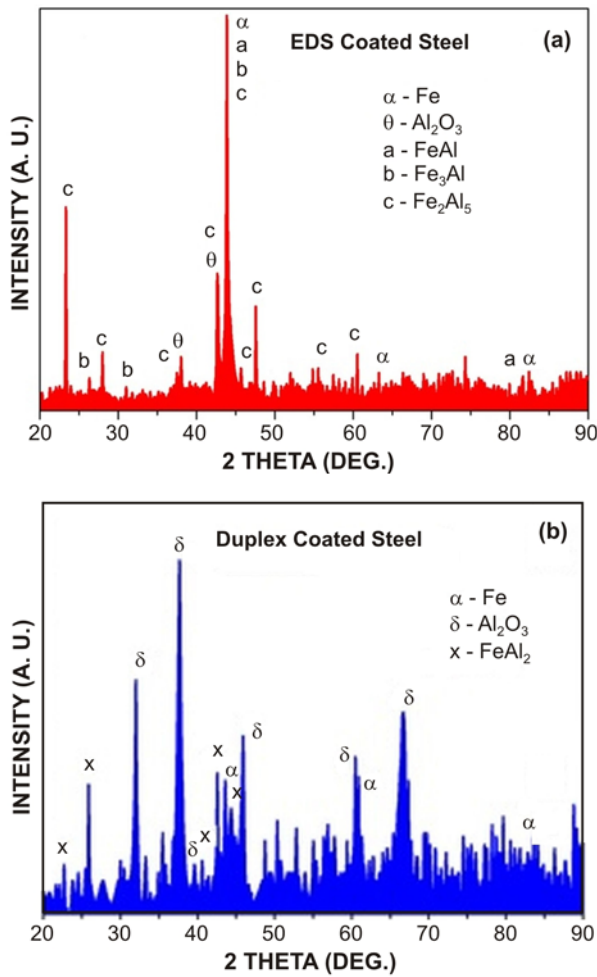
Fig. 4. The XRD patterns of a) the ESD coating and b) the duplex coating.

Fig. 5. The microhardness depth profile of duplex coating on the steel substrate.

The XRD patterns of the ESD coating and the duplex coating are shown in Fig. 4. It can be seen that the XRD patterns of both ESD and duplex coatings have the strong diffraction peaks of Fe since the ESD coating is not so thick on the steel substrate. As it is shown in the XRD patterns, the ESD coating and duplex coating are mainly composed of intermetallics – FeAl, Fe_3Al and Fe_2Al_5 phases and Al_2O_3 phase, respectively. In the present study, the holder fixed aluminum electrode is passed onto the steel substrate manually. Therefore, the electrode should be passing onto the same area on the substrate a few times due to achieving a uniform coating and completely covering the surface. Thus, the coating might have different layers with an initial alloying layer that is rich in iron and poor in aluminum whereas the top layer of coating is rich in aluminum and poor in iron. It is obvious that the top layer will consist of mostly Fe_2Al_5 phase. On the contrary, the initial layer is composed of mostly Fe_3Al phase. It can be concluded that ESD and MAO processes were successfully applied to achieve firstly
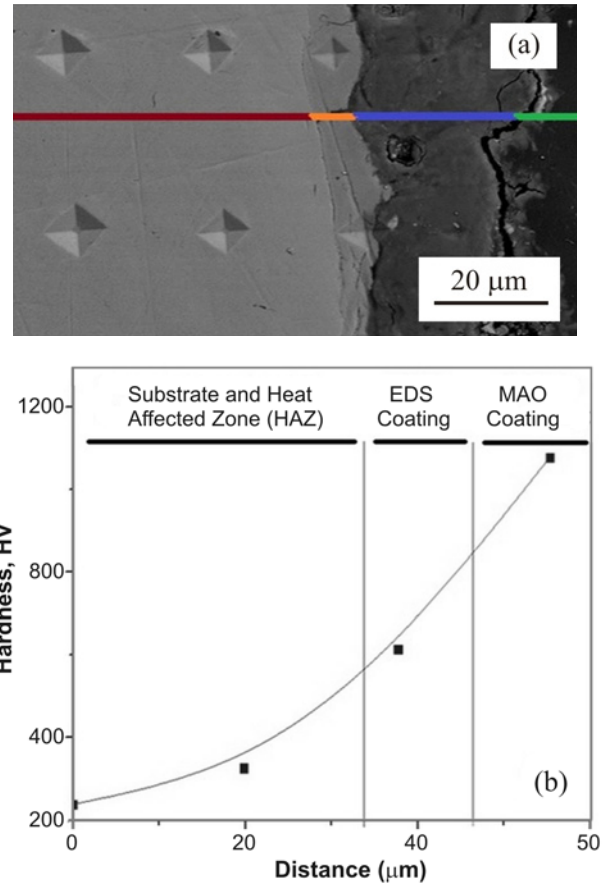
Fe-Al intermetallics and later Al_2O_3 ceramic coatings on the steel substrate.

The SEM micrograph of the cross-section with microhardness indentations and the microhardness distribution along the depth of duplex coating on the steel substrate are presented in Fig. 5. As shown in Fig. 5, the peak value for microhardness reached 1100 HV on the top surface of the duplex coating and was approximately 1.2 times and 5 times higher than that of the ESD coating and the steel substrate, respectively. These results are related to the presence of some phases with high hardness such as Al_2O_3 and Fe-Al intermetallics.

The adhesion characteristics of the ESD and the duplex coatings were investigated with the standard Rockwell-C indentation tests. It is known that the results of Rockwell-C tests are defined for sufficient adhesion as HF-1 to HF-4 and for insufficient as HF-5 and HF-6 [29]. The SEM images of the indents obtained by Rockwell-C tests are shown in Fig. 6. It can be clearly seen that there is neither a delamination nor a radial crack in the indentation of ESD coating. However, in the duplex coating, both cracks and horizontal and/or radial delaminations in the indentation

T a b l e 5. Results of corrosion experiments of the uncoated and coated steel surfaces

Sample	E_{corr} (mV)	i_{corr} (μA cm^{-2})	Corrosion rate (μm year^{-1})
Uncoated steel	−591.7	4.9026	57.34
ESD coated steel	−862.2	4.0463	47.32
Duplex coated steel	−810.6	3.0377	35.53
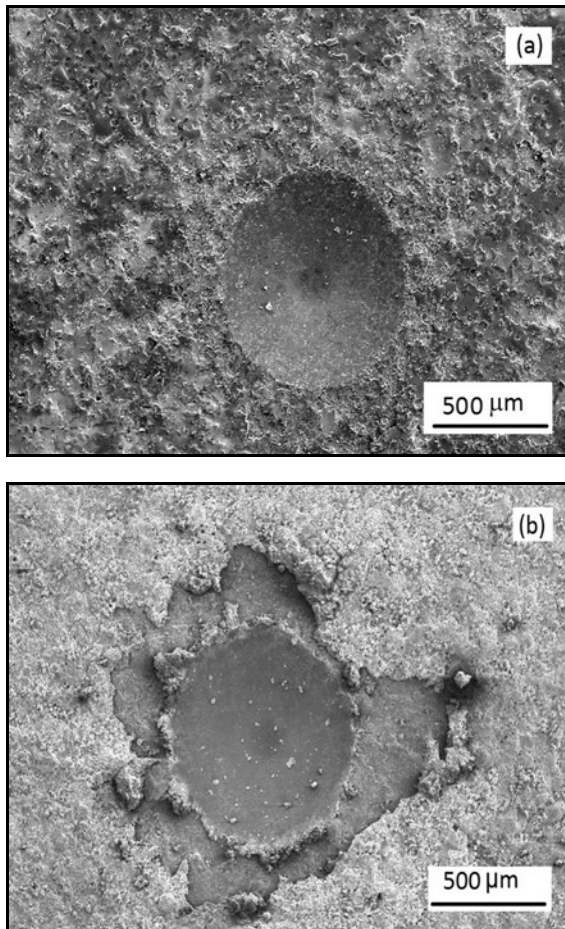
Fig. 6. SEM images of the Rockwell-C indentations of the ESD and duplex coatings.

Fig. 7. The potentiodynamic polarization curves of the uncoated and coated samples.

of the MAO coating duplex could be observed. According to the results, the adhesions of coatings are HF-2 quality for ESD coating and HF-5 quality for MAO layer in the duplex coating. Since ESD coating has a strong metallurgical bonding between the coating and the substrate, it is possible to achieve a sufficient adhesion. However, the duplex coating has an insufficient adhesion because the MAO layer is composed of mainly a ceramic oxide layer (MAO) such as alumina (Al_2O_3), and it leads to brittle behavior.

The electrochemical theory states that the samples with high corrosion potential and low corrosion current density exhibit a low corrosion ra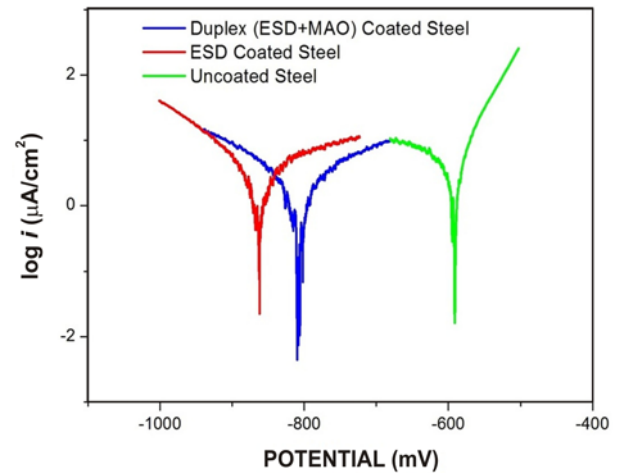te and so they have a good corrosion resistance. The potentiodynamic polarization curves and electrochemical parameters related to these curves of the coated and uncoated samples are presented in Fig. 7 and Table 5, respectively. To get the current-potential diagram, Tafel extrapolation method was used, and the corrosion current (i_{corr}) values were measured by the corrosion equipment, and the corrosion rate was predicted by its software.

According to the corrosion test results, the ESD coated sample with 47.32 μm year^{-1} corrosion rate has much higher (about 20 %) corrosion resistance than the steel substrate with 57.34 μm year^{-1} corrosion rate. Moreover, in the duplex coating, the corrosion resistance was improved about 40 % by using MAO process after ESD process had been applied to the steel substrate. Apparently, the increase in the corrosion resistance of the steel substrate with ESD coated or duplex coated results from the presence of alumina (Al_2O_3) and intermetallic (Fe_3Al and Fe_2Al_5) phases in the microstructures of the coating. However, the present micro-cracks on the coatings affect the behavior corrosion of the samples due to the ions in the NaCl solution diffused easily into the surface of the coatings and could deeply attack the coatings by these micro-cracks during corrosion test. It is concluded that the micro failures in the surface increase the rate of corrosion and so they do not allow increasing the corrosion resistance of the coated samples.

4. Conclusions

It is seen that it is possible to improve surface properties of steel substrates by producing a duplex coating with a combination of electro-spark deposition (ESD) and micro arc oxidation (MAO) processes. The following results can be drawn from the present research:

– It can be understood that it is not possible to increase the coating thickness by increasing the pulse energy (or amplitude of current) in the ESD process in which a couple Al electrode – steel workpiece are used, because the mass transfer is not very effective as the Al element has a melting point much lower than the steel.

– It has been found that the best parameters in terms of mass transfer efficiency were 200 A and 50 µs as the current amplitude and the pulse duration, respectively, in the ESD studies.

– The ESD coating exhibits better adhesion strength than the MAO coating because the ESD process could establish a strong metallurgical bonding between the coating and the substrate.

– While the intermetallic-FeAl, Fe_3Al and Fe_2Al_5 phases are present in the first layer produced by ESD process, an Al_2O_3 phase is detected in the second layer produced by MAO process.

– The presence of these phases in the duplex coating effectively improved the mechanical and corrosion performance of the duplex coated steel substrate. Thus, the microhardness of duplex coating was about 5 times higher than that of the steel substrate, and the corrosion resistance of the duplex coating was about 40 % higher than that of the steel substrate.

Acknowledgements

References

[1] Llewellyn, D. T., Hudd, R. C.: Steels: Metallurgy and Applications. Lincolnshire, Butterworth 1998.
[2] Chang, Y. N., Wei, F. I.: J. Mater. Sci., *24*, 1989, p. 14. doi:10.1007/BF00660927
[3] Schmid, B., Aas, N., Grong, Ø., Ødegård, R.: Oxid. Met., *57*, 2002, p. 115. doi:10.1023/A:1013346813454
[4] Sun, W., Tieu, A. K., Jiang, Z., Lu, C.: J. Mater. Process. Tech., *155–156*, 2004, p. 1307. doi:10.1016/j.jmatprotec.2004.04.167
[5] Melekhov, R. K., Smiyan, O. D., Karvatskyi, L. M., Kapinos, L. V., Lytvyntseva, O. M.: Mater. Sci., *31*, 1995, p. 226. doi:10.1007/BF00558643
[6] Goodwin, G. M.: In: Proceedings of 11th Annual Conference on Fossil Energy Materials. Ed.: Judkins, R. R. Tennessee, US Department of Energy Knoxville 1997, p. 21.
[7] Banovic, S. W., Dupont, J. N., Marder, A. R.: In: Proceedings of 11th Annual Conference on Fossil Energy Materials. Ed.: Judkins, R. R. Tennessee, US Department of Energy Knoxville 1997, p. 27.
[8] Heo, N. H., Kim, M. T., Shin, J. H., Kim, C. Y.: Surf. Coat. Tech., *124*, 2000, p. 39. doi: 10.1016/S0257-8972(99)00519-8
[9] Kumar, S., Selvarajan, V., Padmanabhan, P. V. A., Sreekumar, K. P.: Surf. Coat. Tech., *201*, 2006, p. 1267. doi: 10.1016/j.surfcoat.2006.01.051
[10] Pint, B. A., Leyens, C., Regina, J. R., Tortorelli, P. F., Wright, I. G.: In: Proceedings of 13th Annual Conference on Fossil Energy Materials. Tennessee, Oak Ridge National Laboratory 1999, p. 10.
[11] Grosdidier, T., Tidu, A., Liao, H. L.: Scripta Mater., *44*, 2001, p. 387. doi: 10.1016/S1359-6462(00)00611-4
[12] Guilemany, J. M., Lima, C. R. C., Cinca, N., Miguel, J. R.: Surf. Coat. Tech., *201*, 2006, p. 2072. doi:10.1016/j.surfcoat.2006.04.045
[13] Benamati, G., Buttol, P., Casagrande, A., Fazio, C.: J. Nucl. Mater., *230*, 1996, p. 214. doi: 10.1016/0022-3115(96)80016-X
[14] Christoglou, C., Voudouris, N., Angelopoulos, G. N.: Surf. Coat. Tech., *155*, 2002, p. 51. doi:10.1016/S0257-8972(02)00044-0
[15] Perez, F. J., Duday, D., Hierro, M. P., Gomez, C., Aguero, A., Garcia, M. C., Muela, R., Sanchez Pascual, A., Martinez, L.: Surf. Coat. Tech., *161*, 2002, p. 293. doi: 10.1016/S0257-8972(02)00417-6
[16] Yuh, C., Johnsen, R., Farooque, M., Maru, H.: J. Power Sources, *56*, 1995, p. 1. doi: 10.1016/0378-7753(95)80001-W
[17] Johnson, R. N., Sheldon, G. L.: J. Vac. Sci. Technol., *4*, 1986, p. 2470. doi: 10.1116/1.573672
[18] Agarwal, A., Dahotre, N. B.: Surf. Coat. Tech., *106*, 1998, p. 242. doi: 10.1016/S0257-8972(98)00545-3
[19] Korkmaz, K., Bakan, H. I.: Kovove Mater., *48*, 2010, p. 153. doi: 10.4149/km_2010_2_153
[20] Korkmaz, K.: Surf. Coat. Tech., *272*, 2015, p. 1. doi:10.1016/j.surfcoat.2015.04.033
[21] Frangini, S., Masci, A.: Surf. Coat. Tech., *184*, 2004, p. 31. doi: 10.1016/j.surfcoat.2003.10.050
[22] Johnson, R. N.: In: Proceedings of 9th Annual Conference on Fossil Energy Materials. Tennessee, Oak Ridge National Laboratory 1995, p. 38.
[23] Yerokhin, A. L., Nie, X., Leyland, A., Matthews, A., Dowey, S. J.: Surf. Coat. Tech., *122*, 1999, p. 73. doi: 10.1016/S0257-8972(99)00441-7
[24] Yerokhin, A. L., Nie, X., Leyland, A., Matthews, A.: Surf. Coat. Tech., *130*, 2000, p. 195. doi: 10.1016/S0257-8972(00)00719-2
[25] Durdu, S., Aktuğ, S. L., Korkmaz, K.: Surf. Coat. Tech., *236*, 2013, p. 303. doi: 10.1016/j.surfcoat.2013.10.004
[26] Korkmaz, K.: Surf. Coat. Tech., *272*, 2015, p. 72. doi: 10.1016/j.surfcoat.2015.04.022
[27] Korkmaz, K., Ribalko, A. V., Sahin, O.: Kovove Mater., *51*, 2013, p. 283. doi: 10.4149/km_2013_5_283
[28] Ribalko, A. V., Sahin, O.: Surf. Coat. Tech., *201*, 2006, p. 1724. doi: 10.1016/j.surfcoat.2006.02.044
[29] Heinke, W., Leyland, A., Matthews, A., Berg, G., Friedrich, C.: Thin Solid Films, *270*, 1995, p. 431. doi: 10.1016/0040-6090(95)06934-8
[30] Kaya, S., Demirören, H., Korkut, M. H.: In: Proceedings of XI. International Corrosion Symposium KORSEM'08. Izmir, Dokuz Eylul University 2008.